Design and Implementation of Cosine Control Firing Scheme for Single Phase Fully Controlled Bridge Rectifier

Mukesh Gupta, Sachin Kumar and Vagicharla Karthik

Abstract: As per the industrial needs, regulated dc voltage with linear transfer characteristics is important in many applications such as dc magnet power supplies in a beam line system. To accomplish this motto, cosine control firing scheme is suggested to get the output voltage which is proportional to control voltage. Present paper deals with design and implementation of cosine control firing scheme for single phase fully controlled rectifier with desired results simulated in MATLAB/Simulink and simulation results are verified experimentally.

Keywords: Comparator, cosine control firing scheme, fully controlled bridge rectifier, isolation circuit, monostable multivibrator.

I. INTRODUCTION

Single phase bridge rectifiers utilize thyristor or silicon controlled rectifier (S.C.R.) [1]-[4] as switching devices. To turn on a thyristor, various control schemes are used to generate gate pulses or firing pulses which are supplied between gate and cathode of the thyristor [2]. The number of degrees from the beginning of the cycle when the thyristor is gated or switched on is referred to as the firing angle, α and when the thyristor is turned off is known as extinction angle, β [5], [6]. The thyristors of bridge rectifier are switched on and off in proper sequence by using control electronics and gate driver circuits to get a controlled dc output voltage. For this a sinusoidal ac voltage is supplied to control circuit and the same supply is given to bridge rectifier circuit through isolation and synchronization block as shown in Fig. 1. This paper implements control electronics circuit by using the cosine control firing scheme and the controlled dc output voltage thus obtained from the bridge rectifier is effectively utilized for resistive and motor loads.

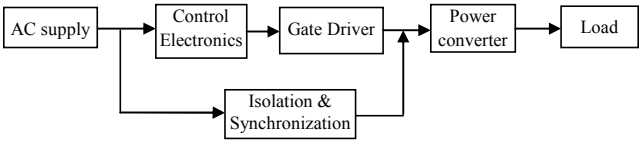

Fig. 1 Typical block diagram of firing angle control scheme.

Mukesh Gupta is working as Assistant Professor in Department of E.E., G.B.P.E.C.-Pauri Garhwal, Uttarakhand. Email: mukesh25071990@gmail.com, Sachin Kumar is working as Assistant Professor in Department of E.E., G.B.P.E.C.-Pauri Garhwal, Uttarakhand. Email: sackumaarc@gmail.com and Vagicharla Karthik is working as Assistant Professor in Department of E.E., G.B.P.E.C.-Pauri Garhwal, Uttarakhand. Email: karthikbec@gmail.com

II. COSINE CONTROL SCHEME

Conventionally, ramp and cosine firing schemes are used for generating the gate pulses [5], [7]. The cosine control firing scheme has an advantage that it linearizes the transfer characteristic of bridge rectifier by using an indirect control variable as a substitute for firing angle, α as given in (1) and (2) [8]. This scheme also provides automatic negative feedback to the change in input ac supply.

The input ac voltage of peak value, V_m is transformed to a low level ac voltage, V_{ao} of 9 V is obtained by using a 230/9 V, 50 Hz step down transformer. The cosine wave generator integrates V_{ao} to obtain a cosine wave of peak value, E_m which is compared with a variable dc control voltage, E_C by using a comparator. The comparator output is fed to monostable block. The monostable output is modulated at high frequency to obtain the firing pulses. After proper amplification and isolation, these firing pulses are supplied to the thyristors of the bridge rectifier circuit.

The firing angle, α is given by

$$\alpha = \cos^{-1}(E_C / E_m) \quad (1)$$

The output voltage of the converter is

$$V_0 = 2V_m / (\pi * \cos\alpha)$$

$$V_0 = 2V_m / (\pi * (E_C / E_m))$$

$$V_0 \propto E_C \quad (2)$$

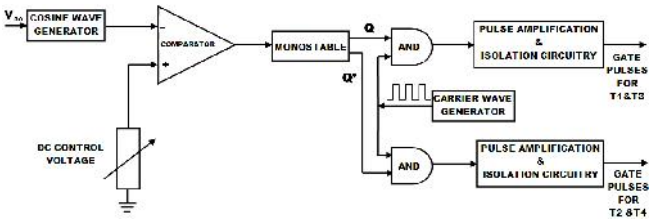

Fig. 2 Block diagram of cosine control scheme.

The block diagram of implemented cosine control firing scheme is shown in Fig. 2 and the utility of each module is explain below [8], [9].

A. Cosine wave generator

Cosine wave generator uses an op-amp along with resistors and capacitors to realize the integrator function. It provides a phase shift of 90^0 to the input voltage V_{a0} and thus a cosine wave is obtained.

B. DC control voltage

The dc control voltage, E_C that can be varied between ± 12 V is used to vary the firing angle, α ranging from 0^0 to 180^0.

The ground point of the dc supply is connected to the common ground point zero of the transformer.

C. Comparator

An op-amp is used as comparator. The variable dc voltage is applied to the non-inverting terminal and the cosine wave is applied to the inverting terminal of the comparator.

D. Monostable

The square wave output of the comparator is fed as input to the monostable multivibrator which gives two complementary outputs, Q and Q' each of 10 ms duration. These complementary outputs are primary firing pulses which are modulated to trigger the thyristors. The time period, T of monostable multivibrator is given in (3).

$$T = 0.33 * R * C \quad (3)$$

where R and C are the resistance and capacitance used.

E. Carrier wave

Pulse gating of thyristor is not suitable for RL loads, this difficulty can be overcome by using continuous gating. However, continuous gating may lead to increased thyristor losses and distortion of output pulse. So, a pulse train generated by modulating the pulse gate at high frequency is used to trigger the thyristor. This high frequency wave is known as carrier wave and is generated by using astable multivibrator.

F. AND

AND operation is performed between monostable outputs and carrier wave thus pulses required for triggering the thyristors called firing pulses or gate pulses are obtained.

G. Pulse amplification and isolation circuitry

The gate pulses obtained from AND operation may not be able to turn on the thyristor [10]. It is therefore common to feed these gate pulses to a pulse amplification and isolation circuitry to meet the two objectives of strengthening these pulses and providing proper isolation.

III. BRIDGE RECTIFIER

The typical single phase bridge rectifier circuit consists of four thyristors T_1, T_2, T_3 and T_4 as shown in Fig. 3. The generated gate pulses are supplied between gate, G and cathode, K to trigger T_1 & T_3 during positive half cycle and T_2 & T_4 during negative half cycle of ac supply voltage [4]. The typical controlled dc output voltage waveforms for resistive and motor loads are shown in Fig. 4 and Fig. 5. The expression of average output voltage, V_0 as a function of firing angle, α and extinction angle, β with resistive load and motor load are given in (4) and (5) respectively.

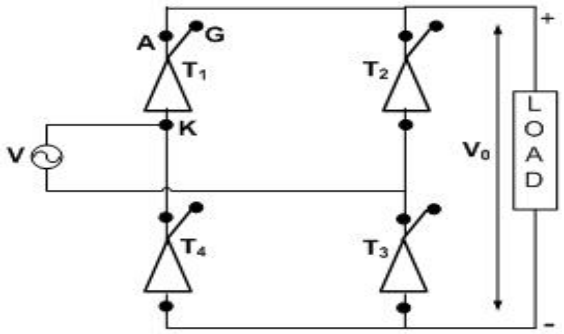

Fig. 3 Typical single phase bridge rectifier circuit diagram.

$$V_0 = \frac{2}{\pi} V_m \cos\alpha \quad (4)$$

$$V_0 = \frac{1}{\pi}[V_m(\cos\alpha - \cos\beta) + E(\pi + \alpha - \beta)] \quad (5)$$

'E' is back e.m.f. of the motor.

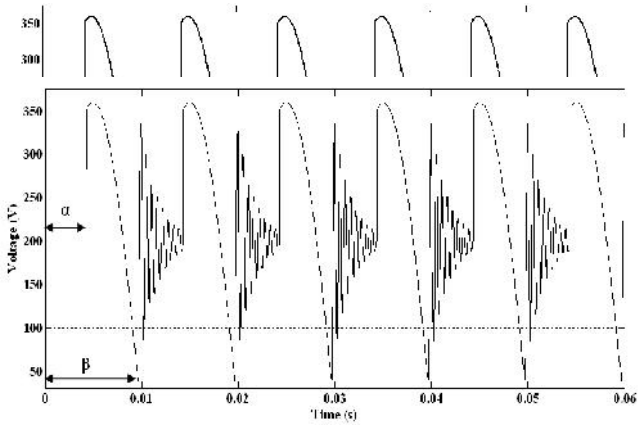

Fig. 4 Typical output waveform of single phase bridge rectifier with resistive load.

Fig. 5 Typical output waveform of single phase bridge rectifier with motor load.

IV. RESULTS

The cosine control firing pulses are supplied to single phase bridge rectifier circuit and the controlled dc output voltage is used to drive the resistive and motor loads.

The voltage waveforms at different stages of control circuit and output of the bridge rectifier circuit as simulated in MATLAB/Simulink are discussed. Afterwards the experimental results are also compared with simulation results.

A. Cosine Control Scheme

a) Cosine wave generator

The simulation results and experimental outputs of the cosine wave generator are shown in Fig. 6 (a) and Fig. 6(b) respectively. The upper half shows an input sine wave and lower half indicates the cosine wave.

b) Comparator

The simulation results and experimental outputs of the comparator are shown in Fig. 7 (a) and Fig. 7 (b) respectively. The lower half shows the square output voltage which is obtained by comparing cosine wave and DC control voltage.

c) Monostable

The square wave output of the comparator is fed to the monostable multivibrator. The simulation results and

experimental outputs of the monostable multivibrator are shown in Fig. 8 (a) and Fig. 8 (b) respectively. The lower and upper halves indicate two output waves each of 10 ms duration and are complement to each other.

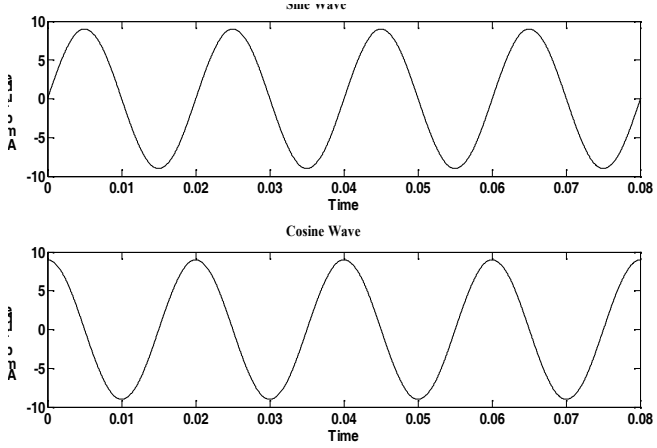

Fig. 6 (a) Simulation results for Input and output of cosine wave generator.

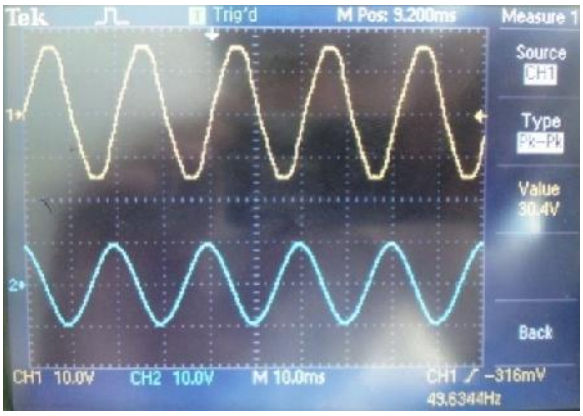

Fig. 6 (b) Experimental results for Input and output of cosine wave generator.

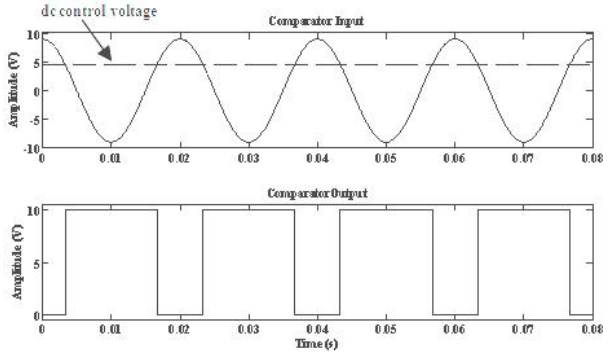

Fig. 7 (a) Simulation results for input and output of comparator.

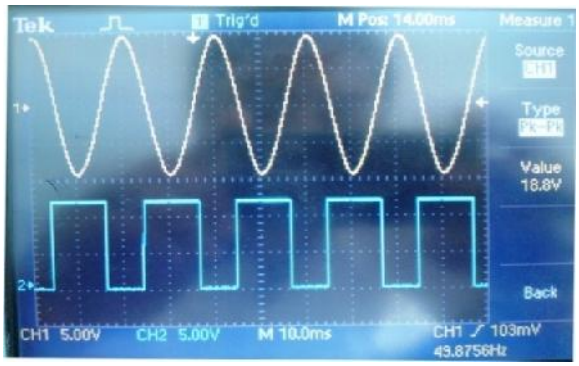

Fig. 7 (b) Experimental results for Input and output of comparator.

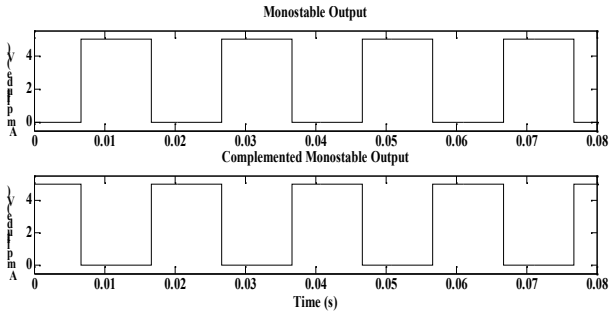

Fig. 8 (a) Simulation results for Input and output of monostable multivibrator.

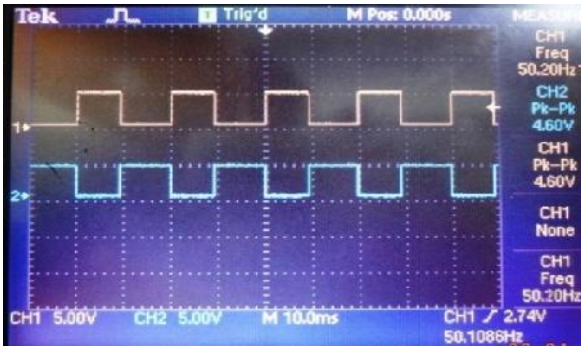

Fig. 8 (b) Experimental results for Input and output of monostable multivibrator.

d) Carrier Wave

The simulation results and experimental outputs of the astable multivibrator are shown in Fig. 9 (a) and Fig. 9 (b) respectively. The output has high frequency pulses of 10 kHz that are used as carrier wave for firing pulses.

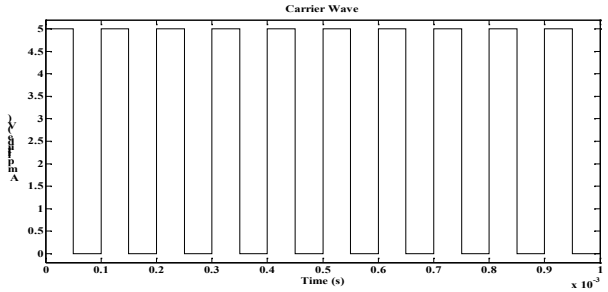

Fig. 9 (a) Simulation results for output of carrier wave generator.

Fig. 9 (b) Experimental results for output of carrier wave

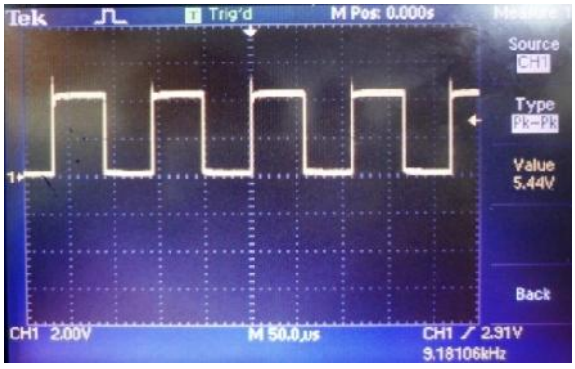

generator.

e) AND Gate

The outputs of the monostable multivibrator are superimposed on the carrier wave using AND operation. The corresponding simulation and experimental results are shown in Fig. 10 (a) and Fig 10 (b) respectively. The lower and upper halves indicate two outputs each of 10 kHz frequency and 10 ms duration and are complement to each other.

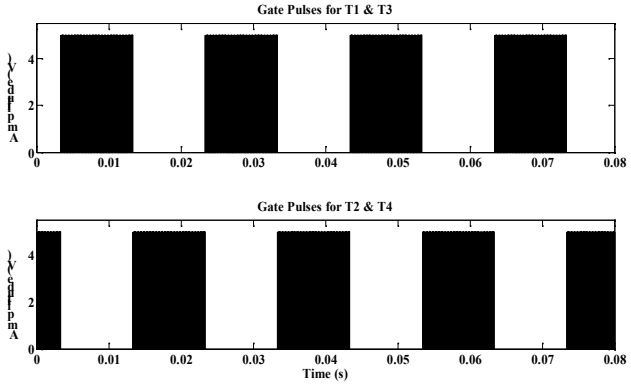

Fig. 10 (a) Simulation results for output of AND operation.

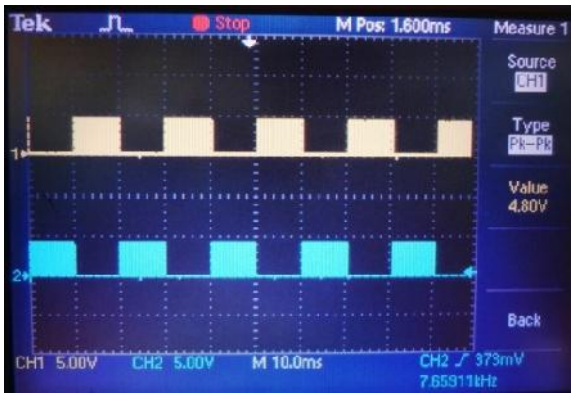

Fig. 10 (b) Experimental results for output of AND operation.

f) *Pulse amplification &Isolation circuitry*

The firing pulses obtained previously are amplified and isolated and experimental results are shown in Fig. 11.

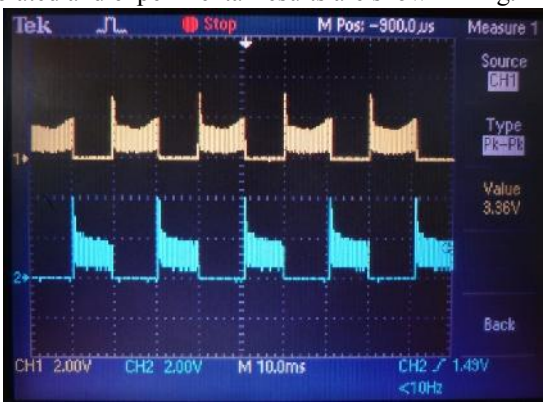

Fig. 11 Experimental results for output of pulse amplification &isolation circuitry.

B. Bridge rectifier output for resistive load

a) for firing angle, α = 76.5^0

The simulation results and experimental outputs of the bridge rectifier with resistive load are shown in Fig. 12 (a) and Fig 12 (b) respectively. The value of average output voltage for simulation as well as for experimental results is given in Table I.

Fig. 12 (a) Simulation result for output of bridge rectifier for

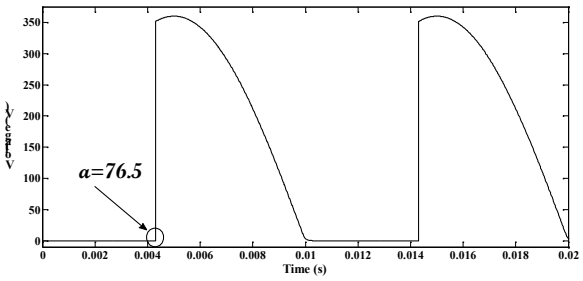

firing angle, α=76.5^0.

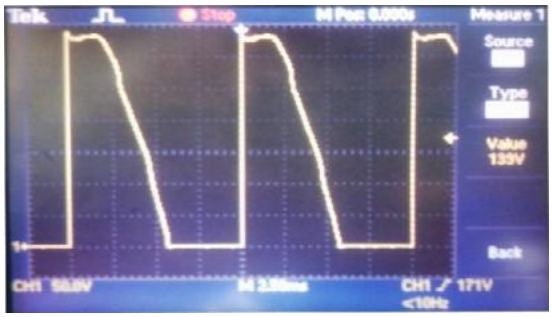

Fig. 12 (b) Experimental result for output of bridge rectifier for firing angle, α=76.5^0.

b) for firing angle, α = 90^0

The simulation results and experimental outputs of the bridge rectifier with resistive load are shown in Fig. 1 (i) and Fig 1(ii) respectively. The value of average output voltage for simulation as well as for experimental results is given in Table I.

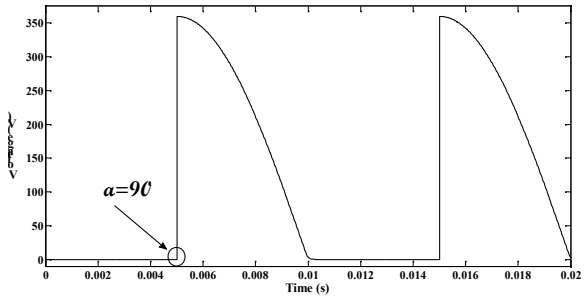

Fig. 13 (a) Simulation result for output of bridge rectifier for firing angle, α=90^0.

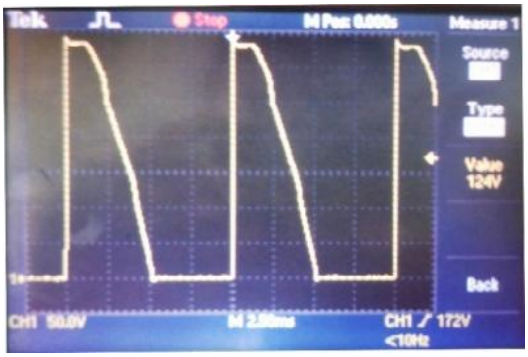

Fig. 13 (b) Experimental result for output of bridge rectifier for firing angle, α=90^0.

c) for firing angle, α = 120⁰

The simulation results and experimental outputs of the bridge rectifier with resistive load are shown in Fig. 14 (a) and Fig. 14 (b) respectively. The value of average output voltage for simulation as well as for experimental results is given in Table I.

It is seen from the above discussion that the theoretical value is slightly less than the practical value which is due to the internal inductance of practical circuit.

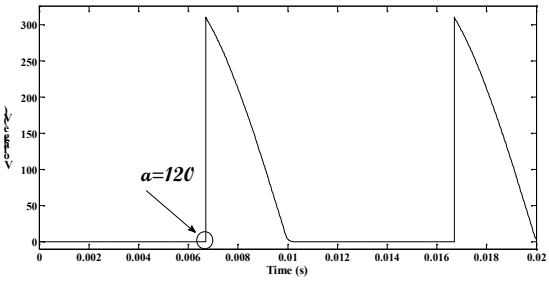

Fig. 14 (a) Simulation result for output of bridge rectifier for firing angle, α=120⁰.

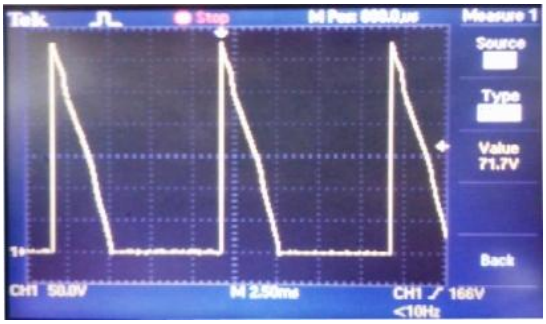

Fig. 14 (b) Experimental result for output of bridge rectifier for firing angle, α=120⁰.

Table I Average output voltage values of bridge rectifier with resistive load

Firing angle, α	Extinction angle, β	Back e.m.f. (E)	V_{0EXP}	V_{0SIM}	Error
76.5⁰	170.1⁰	200 V	222 V	231.60 V	3.89%
90⁰	174.6⁰	200 V	201 V	219.60 V	8.46%
120⁰	189⁰	115 V	121 V	129.30 V	6.41%

C. Bridge rectifier output for motor load

a) for firing angle, α = 76.5⁰

The simulation results and experimental outputs of the bridge rectifier with motor load are shown in Fig. 15 (a) and Fig. 15 (b) respectively. The value of average output voltage for simulation as well as for experimental results is given in Table II.

Fig. 15 (a) Simulation result for output of bridge rectifier for firing angle, α=76.5⁰.

Fig. 15 (b) Experimental result for output of bridge rectifier for firing angle, α=76.5⁰.

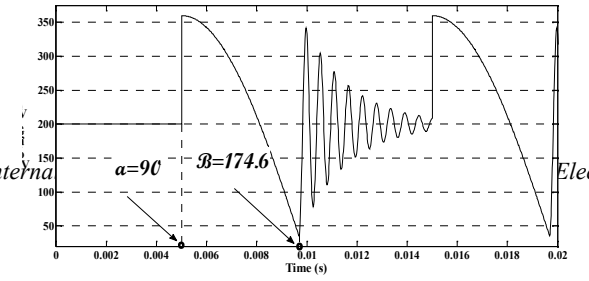

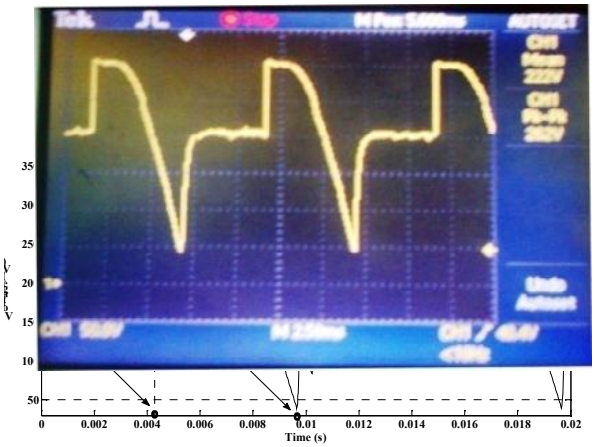

b) for firing angle, α = 90⁰

The simulation results and experimental outputs of the bridge rectifier with motor load are shown in Fig. 16 (a) and Fig. 16 (b) respectively. The value of average output voltage for simulation as well as for experimental results is given in Table II.

Fig. 16 (a) Simulation result for output of bridge rectifier for firing angle, α=90⁰.

Fig. 16 (b) Experimental result for output of bridge rectifier for firing angle, α=90⁰.

c) for firing angle, α = 120⁰

The simulation results and experimental outputs of the bridge rectifier with motor load are shown in Fig. 17 (a) and Fig. 17 (b) respectively. The value of average output voltage for simulation as well as for experimental results is given in Table II.

It is seen from the above discussions that the practical value is slightly less than the theoretical value which is due to the internal inductance of motor.

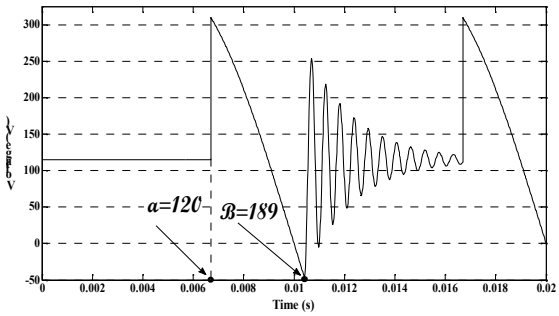

Fig. 17 (a) Simulation result for output of bridge rectifier for firing angle, $\alpha=120^0$.

Fig. 17 (b) Experimental result for output of bridge rectifier for firing angle, $\alpha=120^0$.

Table II Average output voltage values of bridge rectifier with motor load

V_{0EXP} = Experimental Value of Average Voltage

Firing angle, α	Extinction angle, β	Back e.m.f. (E)	V_{0EXP}	V_{0SIM}	Error
76.5^0	170.1^0	200 V	222 V	231.60 V	3.89%
90^0	174.6^0	200 V	201 V	219.60 V	8.46%
120^0	189^0	115 V	121 V	129.30 V	6.41%

V_{0SIM} = Simulation Value of Average Voltage

V. CONCLUSION

Gate pulses obtained by cosine control scheme have been effectively utilized to control the dc output single phase fully controlled bridge rectifier on both resistive load and motor load. The present control scheme provides linear control transfer characteristics between input and output i.e., firing angle is directly proportional to the dc control voltage. The experimental results are in coordination with the simulation results. Thus, presented control scheme can be successfully utilized to get the controlled dc voltage for industrial applications.

In order to produce steady and smooth DC, a filter may be introduced at the output [7]. Pulse amplification and isolation circuitry may be replaced by driver ICs.

Monostable are may be replaced by zero-crossing detector and AND gates to avoid the false triggering due to output bouncings [11].

APPENDIX

List of components and tools used

1. **For control circuit:**
   a) Transformers: 230v/9v, 230 v/ 12-0-12 v, 230v/6v and 230v/12v.
   b) op amp IC 741
   c) monostable IC 74123
   d) timer IC 555
   e) AND IC 7408
   f) Diodes IN4007
   g) Zener diode 5.1V

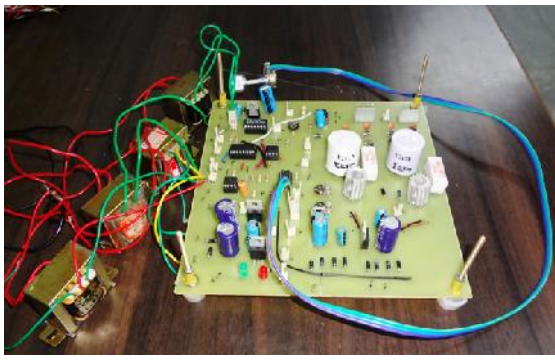

   h) Regulator ICs 7812, 7912, and 7805
   i) SL100 transistors
   j) Pulse Transformer 4503
   k) Resistors and capacitors of various values External pots and internal pots.
   l) Heat Sinks
2. **For bridge rectifier circuit:**
   a) Thyristors TYN612
   b) Power diodes IN 5408
   c) Heat Sinks
   d) Resistors and capacitors
3. **Tools:**
   a) Incandescent bulb
   b) DC motor
   c) Bread board
   d) Connecting wires
   e) Printed Circuit Board
   f) Wire Cutter
   g) Long Nose Pliers
   h) DC Power Supply
   i) AC Power Supply
   j) Two channel oscilloscope
   k) Differential probe
   l) Digital multimeter

Fig. A1 Printed circuit board for control and bridge rectifier circuits.

Fig. A2 Practical Control Circuit.

Fig. A3 Control and bridge rectifier circuits with resistive load.

Fig. A4 Control and bridge rectifier circuits with motor load.

ACKNOWLEDGMENT

Authors whole heartedly thank to G.B. Pant Engineering College for providing an opportunity to compose an international journal paper on thyristor firing which is emerging trend in power electronics. Authors take this opportunity to express their gratitude towards Mr. V.M. Mishra (Head of Electrical Engineering Department, G.B.P.E.C. Pauri) for providing us the valuable facilities. Authors would like to thank all their colleagues for their support. Last but not least authors would like to thank all the departments of G.B.P.E.C. Pauri for their physical, emotional and intellectual support especially precious suggestions in need.

REFERENCES

[1] P. S. Bimbhra, "Power Electronics," Khanna Publishers, 3rd edition pp. 62-72 and 176-179, 2006.

[2] P. C. Sen, "Power Electronics," Tata McGraw Hill Publishers, 4th edition pp. 21-49 and 83-91, 1987.

[3] Muhammad H. Rashid, "Power Electronics," Prentice Hall of India Publication, 4th edition, 2009.

[4] N. Mohan, T. M. Undeland and W. P. Robbins, "Power Electronics: Converters. Applications, and Design," New York: Wiley, 3rd edition pp. 122-128, 2006.

[5] Tirtharaj Sen, Pijush Kanti Bhattacharjee and Manjima Bhattacharya, "Design And Implementation Of Firing Circuit For Single- Phase Converter," International Journal of Computer and Electrical Engineering, vol. 3, pp. 368-374, June 2011.

[6] Philip T. Krein, "Elements of Power Electronics," 4th edition Oxford University Press, 2003.

[7] Ahmad Azhar Bin Awang, "Single Phase Controlled Rectifier Using Thyristor," undergraduate thesis, Universiti Teknologi Malaysia, 2009-10.

[8] Geno Peter, "Design Of Single Phase Fully Controlled Converter Using Cosine Wave Crossing Control With Various Protections," International Journal of Engineering Science and Technology, vol. 2(9), pp 4222-4227, 2010.

[9] Paul B. Zbar and Albert P. Malvino, "Basic Electronics: A Text – Lab Manual," Tata McGraw-Hill Publisher, 7th edition, 2001.

[10] O. P. Arora, "Power Electronics Laboratory: Experiments & Organization", Wheeler Publishing , 1st edition, 1993.

[11] Yu-Kang Lo and Chem-Lin Chen, "An Improved Cosine-Mode Controller for SCR Converters," IEEE transactions on Industrial Electronics, vol. 42, pp. 552-554, October 1995.

Mukesh Gupta is a recent graduate of B.Tech. in Electrical Engineering from G.B. Pant Engineering College, Pauri-Garhwal India 246194. He is a Gold-Medalist in Electrical Engineering from Uttarakhand Technical University, Dehradun. He is a member of Indian Society for Technical Education (I.S.T.E.). His area of interest is electrical machine, drives and power system.

Sachin Kumar is Assistant Professor of Electrical Engineering with G.B. Pant Engineering College, Pauri-Garhwal 246194 India. He received his Masters Degree from I.I.T. Kharagpur in 2010. He has published four papers in Electrical and Electronics Engineering. His area of interest is high voltage insulation and testing.

Vagicharla Karthik is Assistant Professor of Electrical Engineering with G.B. Pant Engineering College, Pauri-Garhwal 246194 India. He received his Masters Degree from I.I.T. Roorkee in 2010. He has published six papers in Electrical and Electronics Engineering. His area of interest is electrical machine and drives and F.P.G.A.